

Capability of LHC to discover supersymmetry with $\sqrt{s}=7$ TeV and 1 fb^{-1}

Howard Baer^a, Vernon Barger^b, Andre Lessa^a and Xerxes Tata^{b,c}

^a*Dept. of Physics and Astronomy, University of Oklahoma, Norman, OK 73019, USA*

^b*Dep't of Physics, University of Wisconsin, Madison, WI 53706, USA*

^c*Dept. of Physics and Astronomy, University of Hawaii, Honolulu, HI 96822, US*

E-mail: baer@nhn.ou.edu, barger@pheno.wisc.edu, lessa@nhn.ou.edu, tata@phys.hawaii.edu

ABSTRACT: We examine the capability of the CERN Large Hadron Collider to discovery supersymmetry (SUSY) with energy $\sqrt{s} = 7$ TeV and integrated luminosity of about 1 fb^{-1} . Our results are presented within the paradigm minimal supergravity model (mSUGRA or CMSSM). Using a 6-dimensional grid of cuts for optimization of signal to background—including missing E_T —we find for $m_{\tilde{g}} \sim m_{\tilde{q}}$ an LHC reach of $m_{\tilde{g}} \sim 800, 950, 1100$ and 1200 GeV for $0.1, 0.3, 1$ and 2 fb^{-1} , respectively. For $m_{\tilde{g}} \ll m_{\tilde{q}}$, the reach is instead near $m_{\tilde{g}} \sim 480, 540, 620$ and 700 GeV, for the same integrated luminosities. We also examine the LHC reach in the case of very low integrated luminosity where missing E_T may not be viable. We focus on the multi-muon, multi-lepton (including electrons) and dijet signals. Although the LHC reach without E_T^{miss} is considerably lower in these cases, it is still substantial: for 0.3 fb^{-1} , the dijet reach in terms of gluino mass is up to 600 GeV for very low m_0 , while the dilepton reach is to gluino masses of ~ 500 GeV over a range of m_0 values.

KEYWORDS: Supersymmetry Phenomenology, Supersymmetric Standard Model, Large Hadron Collider.

1. Introduction

The CERN Large Hadron Collider (LHC) has recently begun to generate data from proton-proton collisions at $\sqrt{s} = 7$ TeV. The plan is to run for much of the next two years, with a goal of accumulating $\sim 1 \text{ fb}^{-1}$ of usable data. This initial run will be followed by a shut down for a year or so for various upgrades, followed by a turn-on at or near design energy of $\sqrt{s} = 14$ TeV.

The discovery capability of LHC with $\sqrt{s} = 14$ TeV (LHC14), has been investigated for several new physics scenarios, where supersymmetry (SUSY) [1] is frequently used as a canonical example [2]. In the paradigm minimal supergravity (mSUGRA or CMSSM) model [3] based on local supersymmetry [4], the LHC14 reach with 100 fb^{-1} was found to extend to $m_{\tilde{g}} \sim 3.1$ TeV for $m_{\tilde{q}} \sim m_{\tilde{g}}$, and to $m_{\tilde{g}} \sim 1.8$ TeV, for $m_{\tilde{q}} \gg m_{\tilde{g}}$.

As LHC turn-on drew near, the question turned to how well LHC could do in its initial stages, at very low integrated luminosity, and perhaps before the LHC detectors are fully calibrated, so that the canonical SUSY signature – the presence of multi-jet plus large missing E_T (E_T^{miss}) – is not fully viable. In Ref. [5, 6, 7], it was emphasized that SUSY could be discovered at LHC even without using E_T^{miss} , by focusing instead on events with large multiplicity of isolated leptons. In Ref. [6], it was shown that LHC could discover SUSY in the dijet channel, using new kinematic variables, even without viable E_T^{miss} .

In a previous study [7], we investigated the supersymmetry discovery potential of LHC with $\sqrt{s} = 10$ TeV (LHC10), the energy at which the machine was then expected to operate, both with and without the use of E_T^{miss} , and compared it to the reach of LHC14. After Ref. [7] appeared, the decision was made to operate LHC at half its design energy of $\sqrt{s} = 7$ TeV (LHC7). Furthermore, the additional year of LHC down-time allowed the various detectors to amass millions of cosmic muon events. This array of cosmic data allowed the experiments to make progress on important issues of detector alignment, tracking and calibration. At the end of 2009, the first proton-proton collisions were recorded in the CMS and ATLAS (and ALICE and LHC-b) detectors at center-of-mass energies of 900 GeV and 2.36 TeV. Initial analyses of these events show remarkably good agreement between Monte Carlo expectations and the actual data, including the (very low energy) E_T^{miss} spectrum [8, 9]. By March 30, 2010, the first pp collisions were recorded at $\sqrt{s} = 7$ TeV. At this time, millions of pp collision events at 7 TeV have been recorded, including various multi-jet events, and even candidate leptonically decaying W events.

In light of the CERN decision to perform a major collider run at $\sqrt{s} = 7$ TeV with $\sim 1 \text{ fb}^{-1}$ of integrated luminosity, it is reasonable to re-calculate the SUSY reach using the revised run parameters. In this paper, we evaluate the discovery capability of LHC7 for SUSY particles and display it as a reach plot in the $m_0 - m_{1/2}$ plane of the mSUGRA model. The parameter space of the model is given by

$$m_0, m_{1/2}, A_0, \tan \beta, \text{sign}(\mu), \quad (1.1)$$

where m_0 is a common GUT scale soft SUSY breaking (SSB) scalar mass, $m_{1/2}$ is a common GUT scale SSB gaugino mass, A_0 is a common GUT scale trilinear SSB term, $\tan \beta$ is the

ratio of Higgs field vevs, and μ is the superpotential Higgs mass term, whose magnitude, but not sign, is constrained by the electroweak symmetry breaking minimization conditions.

At each model parameter space point, many simulated collider events are generated and compared against SM backgrounds with the same experimental signature [10]. A 6-dimensional grid of cuts are then employed to enhance the SUSY signal over SM backgrounds, and the signal is deemed observable if it satisfies pre-selected criteria for observability. Based on previous studies [2], we include in our analysis the following channels:

- $jets + E_T^{\text{miss}}$ (no isolated leptons),
- $1\ell + jets + E_T^{\text{miss}}$,
- two opposite-sign isolated leptons (OS)+ $jets + E_T^{\text{miss}}$,
- two same-sign isolated leptons (SS)+ $jets + E_T^{\text{miss}}$,
- $3\ell + jets + E_T^{\text{miss}}$.

We evaluate the reach for various values of integrated luminosities ranging from 0.1 fb^{-1} to 2 fb^{-1} , that may be relevant at LHC7.

While the initial reports of detector performance at $\sqrt{s} \sim 0.95 - 2.36 \text{ TeV}$ are encouraging, we should keep in mind that the initial agreement between data and event simulation has been obtained at low luminosity and CM energies, and only for relatively simple event topologies with $E_T^{\text{miss}} \lesssim 40 \text{ GeV}$ and with limited total scalar E_T in the events. Since fake E_T^{miss} grows with the total scalar energy in hadron collider events, it is still unclear how accurate the E_T^{miss} measurements will be at very high values of $E_T^{\text{miss}} \sim 100 - 500 \text{ GeV}$. With this in mind, we include a separate conservative low luminosity reach analysis where we do not make use of any E_T^{miss} information. We also present results with only reliable isolated muon identification,¹ since misidentification of jets as electrons could be problematic at very early stages in the analysis. We also present our no- E_T^{miss} results in the case where both e s and μ s are reliably identified. In these cases, with limited detector performance the LHC reach, though more limited, still extends considerably beyond present limits.

The remainder of this paper is organized as follows. In Sec. 2, we present details of our SUSY signal and SM background calculations. In Sec. 3, we show LHC7 reach plots using the complete anticipated detector performance, including reliable E_T^{miss} resolution and electron ID, for integrated luminosities from $0.1\text{-}2 \text{ fb}^{-1}$. Our full analysis plots include scans over a vast grid of possible cut values, so signal/background is optimized in various regions of model parameter space. In Sec. 4, we present SUSY discovery reach plots in the more conservative scenario where reliable E_T^{miss} measurement may not be attainable, including the case that reliable e ID may also not yet be possible. We also show reach results for acollinear dijet production via the Randall-Tucker-Smith analysis [6]. We conclude with a summary of our results in Sec. 5.

¹Both ATLAS and CMS have already recorded and analysed large numbers of cosmic ray muons. This muon data has served to calibrate and align the detector subsystems. Moreover, muons can be identified down to lower p_T values than electrons.

2. Standard model background and signal calculations

Because our analysis covers several search channels, we include in our background calculations all relevant $2 \rightarrow n$ processes for the multi-lepton and multi-jet searches. However, since we restrict our results to the first LHC physics run ($\lesssim 2 \text{ fb}^{-1}$ and $\sqrt{s} = 7 \text{ TeV}$) we can ignore processes such as $pp \rightarrow VVV$ ($V = W^\pm, Z$), for which the cross section is too small to be relevant. In order to obtain a proper statistical representation of our background and signal events, we generate (at least) the equivalent of 1 fb^{-1} of events for each process (except for our QCD samples).

For the simulation of the background events, we use AlpGen and MadGraph to compute the hard scattering events and Pythia [11] for the subsequent showering and hadronization. For the final states containing multiple jets (namely $Z(\rightarrow ll, \nu\nu) + jets$, $W(\rightarrow l\nu) + jets$, $b\bar{b} + jets$, $t\bar{t} + jets$, $Z + b\bar{b} + jets$, $Z + t\bar{t} + jets$, $W + b\bar{b} + jets$, $W + t\bar{t} + jets$ and QCD), we use the MLM matching algorithm [12] to avoid double counting. All the processes included in our analysis are shown in Table 1 as well as their total cross-sections, number of events generated and event generator used. The signal events were generated using Isajet 7.79 [13] which, given an mSUGRA parameter set, generates all $2 \rightarrow 2$ SUSY processes in the right proportion, and decays the sparticles to lighter sparticles using the appropriate branching ratios and decay matrix elements, until the sparticle decay cascade terminates in the stable LSP, assumed here to be the lightest neutralino.

Using Prospino [14], we plot in Fig. 1 the NLO gluino and squark production cross-sections for the LHC at 7 TeV for the case of a) $m_{\tilde{q}} = m_{\tilde{g}}$ and b) $m_{\tilde{q}} = 2m_{\tilde{g}}$. In frame a), we see that for low $m_{\tilde{g}} \lesssim 500 \text{ GeV}$, the total strongly interacting sparticle pair production cross section exceeds 10^4 fb , so that with 1 fb^{-1} of integrated luminosity, there could be cases where over 10^4 sparticle pair production events are created at LHC during the first run! For $m_{\tilde{q}} \sim m_{\tilde{g}}$, $\tilde{q}\tilde{g} + \tilde{q}\tilde{q}$ production are the dominant sparticle production mechanisms, whereas for $m_{\tilde{q}} \sim 2m_{\tilde{g}}$ the total SUSY cross section is dominated by $\tilde{g}\tilde{g}$ production and is somewhat smaller.

For event generation, we use a toy detector simulation with calorimeter cell size $\Delta\eta \times \Delta\phi = 0.05 \times 0.05$ and $-5 < \eta < 5$. The HCAL (hadronic calorimetry) energy resolution is taken to be $80\%/\sqrt{E} + 3\%$ for $|\eta| < 2.6$ and FCAL (forward calorimetry) is $100\%/\sqrt{E} + 5\%$ for $|\eta| > 2.6$, where the two terms are combined in quadrature. The ECAL (electromagnetic calorimetry) energy resolution is assumed to be $3\%/\sqrt{E} + 0.5\%$. We use the cone-type Isajet [13] jet-finding algorithm to group the hadronic final states into jets. Jets and isolated lepton are defined as follows:

- Jets are hadronic clusters with $|\eta| < 3.0$, $R \equiv \sqrt{\Delta\eta^2 + \Delta\phi^2} \leq 0.4$ and $E_T(jet) > 50 \text{ GeV}$.
- Electrons and muons are considered isolated if they have $|\eta| < 2.0$, $p_T(l) > 10 \text{ GeV}$ with visible activity within a cone of $\Delta R < 0.2$ about the lepton direction, $\Sigma E_T^{cells} < 5 \text{ GeV}$.
- We identify hadronic clusters as b -jets if they contain a B hadron with $E_T(B) > 15 \text{ GeV}$, $\eta(B) < 3$ and $\Delta R(B, jet) < 0.5$. We assume a tagging efficiency of 60% and

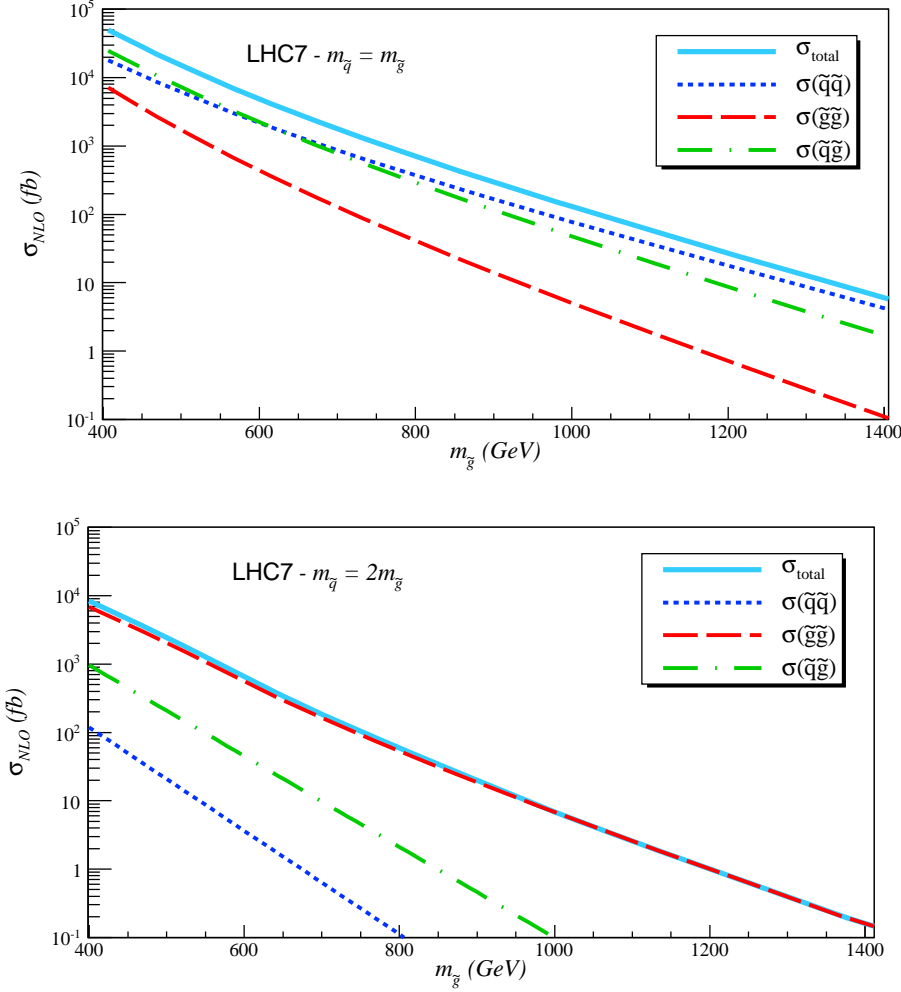


Figure 1: Squark and gluino production cross-sections at NLO for LHC7 as a function of $m_{\tilde{g}}$. In frame a) we show the cross-sections for $m_{\tilde{q}} = m_{\tilde{g}}$, while frame b) has $m_{\tilde{q}} = 2m_{\tilde{g}}$.

light quark and gluon jets can be mis-tagged as a b -jet with a probability $1/150$ for $E_T \leq 100$ GeV, $1/50$ for $E_T \geq 250$ GeV, with a linear interpolation for $100 \text{ GeV} \leq E_T \leq 250$ GeV

We point out the following technical improvements to our previous analyses [7]:

- QCD events are now generated in E_T bins for the hardest jet; this gives a better statistical representation for the high $E_T(j)$ events.
- Our current analysis uses Isajet 7.79 for event generation. The version 7.79 SUSY spectrum calculation includes threshold corrections at each distinct decoupling squark and slepton mass value, whereas previous Isajet versions implemented all squark threshold corrections at a common scale $m_{\tilde{u}_L}$ and all sleptons at a common scale $m_{\tilde{e}_L}$ [15]. Furthermore, previous Isajet versions included two-loop RGE running for the

SM process	Generator	Cross section	number of events
QCD: 2, 3 and 4 jets ($40 \text{ GeV} < E_T(j1) < 100 \text{ GeV}$)	AlpGen	$2.6 \times 10^9 \text{ fb}$	26M
QCD: 2, 3 and 4 jets ($100 \text{ GeV} < E_T(j1) < 200 \text{ GeV}$)	AlpGen	$3.9 \times 10^8 \text{ fb}$	44M
QCD: 2, 3 and 4 jets ($200 \text{ GeV} < E_T(j1) < 500 \text{ GeV}$)	AlpGen	$1.6 \times 10^7 \text{ fb}$	16M
QCD: 2, 3 and 4 jets ($500 \text{ GeV} < E_T(j1) < 3000 \text{ GeV}$)	AlpGen	$9.4 \times 10^4 \text{ fb}$	0.3M
$t\bar{t}$: $t\bar{t} + 0, 1$ and 2 jets	AlpGen	$1.6 \times 10^5 \text{ fb}$	5M
$b\bar{b}$: $b\bar{b} + 0, 1$ and 2 jets	AlpGen	$8.8 \times 10^7 \text{ fb}$	91M
$Z + \text{jets}$: $Z/\gamma(\rightarrow l\bar{l}, \nu\bar{\nu}) + 0, 1, 2$ and 3 jets	AlpGen	$8.6 \times 10^6 \text{ fb}$	13M
$W + \text{jets}$: $W^\pm(\rightarrow l\nu) + 0, 1, 2$ and 3 jets	AlpGen	$1.8 \times 10^7 \text{ fb}$	19M
$Z + t\bar{t}$: $Z/\gamma(\rightarrow l\bar{l}, \nu\bar{\nu}) + t\bar{t} + 0, 1$ and 2 jets	AlpGen	53 fb	0.6M
$Z + b\bar{b}$: $Z/\gamma(\rightarrow l\bar{l}, \nu\bar{\nu}) + b\bar{b} + 0, 1$ and 2 jets	AlpGen	$2.6 \times 10^3 \text{ fb}$	0.3M
$W + b\bar{b}$: $W^\pm(\rightarrow \text{all}) + b\bar{b} + 0, 1$ and 2 jets	AlpGen	$6.4 \times 10^3 \text{ fb}$	9M
$W + t\bar{t}$: $W^\pm(\rightarrow \text{all}) + t\bar{t} + 0, 1$ and 2 jets	AlpGen	$1.8 \times 10^2 \text{ fb}$	9M
$W + tb$: $W^\pm(\rightarrow \text{all}) + t\bar{b}(t\bar{b})$	AlpGen	$6.8 \times 10^2 \text{ fb}$	0.025M
$t\bar{t}t\bar{t}$	MadGraph	0.6 fb	1M
$t\bar{t}b\bar{b}$	MadGraph	$1.0 \times 10^2 \text{ fb}$	0.2M
$b\bar{b}b\bar{b}$	MadGraph	$1.1 \times 10^4 \text{ fb}$	0.07M
WW : $W^\pm(\rightarrow l\nu) + W^\pm(\rightarrow l\nu)$	AlpGen	$3.0 \times 10^3 \text{ fb}$	0.005M
WZ : $W^\pm(\rightarrow l\nu) + Z(\rightarrow \text{all})$	AlpGen	$3.4 \times 10^3 \text{ fb}$	0.009M
ZZ : $Z(\rightarrow \text{all}) + Z(\rightarrow \text{all})$	AlpGen	$4.0 \times 10^3 \text{ fb}$	0.02M

Table 1: Background processes included in this LHC7 study, along with their total cross sections and number of generated events. All light (and b) partons in the final state are required to have $E_T > 40 \text{ GeV}$. For QCD, we generate the hardest final parton jet in distinct bins to get a better statistical representation of hard events. For Wtb production, additional multi-jet production is only via the parton shower because the AlpGen calculation including all parton emission matrix elements is not yet available. For this process, we apply the cut $|m(Wb) - m_t| \geq 5 \text{ GeV}$ to avoid double counting events from real $t\bar{t}$ production.

MSSM only from the M_{SUSY} scale up to M_{GUT} ; Isajet 7.79 also includes two-loop RGE running from M_Z up to M_{SUSY} (for more details see Ref. [16]).

- We consider b -jet tagging to improve the optimized reach of the LHC.

3. Optimized reach of the LHC utilizing E_T^{miss}

As noted in Sec. 1, preliminary results from minimum bias events in pp collisions at $\sqrt{s} = 0.9$ and 2.36 TeV already show good reconstruction of the E_T^{miss} spectrum for low missing E_T out to $E_T^{\text{miss}} \sim 35 \text{ GeV}$. As the experiments accumulate data, the reconstruction algorithms will be fully tested and refined, and soon E_T^{miss} should become a reliable variable for detecting SUSY events. With this in mind, we examine the SUSY reach of LHC7 including E_T^{miss} and also isolated electrons in the analysis, even for small integrated luminosities. Certainly by the time the integrated luminosity exceeds $\sim 0.5 - 1 \text{ fb}^{-1}$, we

expect the detector to be very well understood, leading us to optimize the reach by looking simultaneously at various multi-jets and multi-lepton channels.

As in Ref. [7], we define the signal to be observable if

$$S \geq \max \left[5\sqrt{B}, 5, 0.2B \right]$$

where S and B are the expected number of signal and background events, respectively, for an assumed value of integrated luminosity. The requirement $S \geq 0.2B$ is imposed to avoid the possibility that a *small* signal on top of a *large* background could otherwise be regarded as statistically significant, but whose viability would require the background level to be known with exquisite precision in order to establish a discovery. Our optimization procedure selects the channel which maximizes $S/\sqrt{S+B}$, used as the figure of merit for the statistical significance of the signal.

The grid of cuts used in our optimized analysis is:

- $E_T^{\text{miss}} > 100 - 1000$ GeV (in steps of 100 GeV),
- $n(\text{jets}) \geq 2, 3, 4, 5$ or 6,
- $n(b - \text{jets}) \geq 0, 1, 2$ or 3,
- $E_T(j_1) > 50 - 300$ GeV (in steps of 50 GeV) and 400-1000 GeV (in steps of 100 GeV) (jets are ordered $j_1 - j_n$, from highest to lowest E_T),
- $E_T(j_2) > 50 - 200$ GeV (in steps of 30 GeV) and 300, 400, 500 GeV,
- $n(\ell) = 0, 1, 2, 3$, OS, SS and inclusive channel: $n(\ell) \geq 0$. (Here, $\ell = e, \mu$).
- $10 \text{ GeV} \leq m(\ell^+\ell^-) \leq 75 \text{ GeV}$ or $m(\ell^+\ell^-) \geq 105 \text{ GeV}$ (for the OS, same flavor (SF) dileptons only),
- transverse sphericity $S_T > 0.2$.

We show in Fig. 2 the optimized discovery reach of LHC7. We also show gluino isomass curves and the SM Higgs mass bound contours as obtained using the Isasugra routines in Isajet, together with contours of $m_h = 111$ and 114 GeV. While limits from Higgs searches at LEP2 imply $m_h > 114.4$ GeV for a SM-like Higgs boson, we also show the $m_h \sim 111$ GeV contour as a conservative indicator of the Higgs limit in the mSUGRA model to incorporate an approximate ± 3 GeV uncertainty in the theoretical calculation of m_h .

We see in Fig. 2 that with only 0.1 fb^{-1} of integrated luminosity, experiments at the LHC will be able to explore well beyond current Tevatron bounds, reaching $m_{\tilde{g}} \sim 800$ GeV for $m_{\tilde{q}} \simeq m_{\tilde{g}}$ in the low m_0 part of the figure. The precise reach will be determined by background levels in different channels (many of which will be able to be obtained directly from the data as discussed in Ref. [7]). The gluino mass reach for $m_{\tilde{g}} \sim m_{\tilde{q}}$ extends up to 950 (1100) ((1200)) GeV for 0.3 (1) ((2)) fb^{-1} of integrated luminosity, respectively! For heavy squarks (large m_0 region), the reach is still at the level of $m_{\tilde{g}} \simeq 540$ (650) ((700)) GeV for 0.3 (1) ((2)) fb^{-1} .

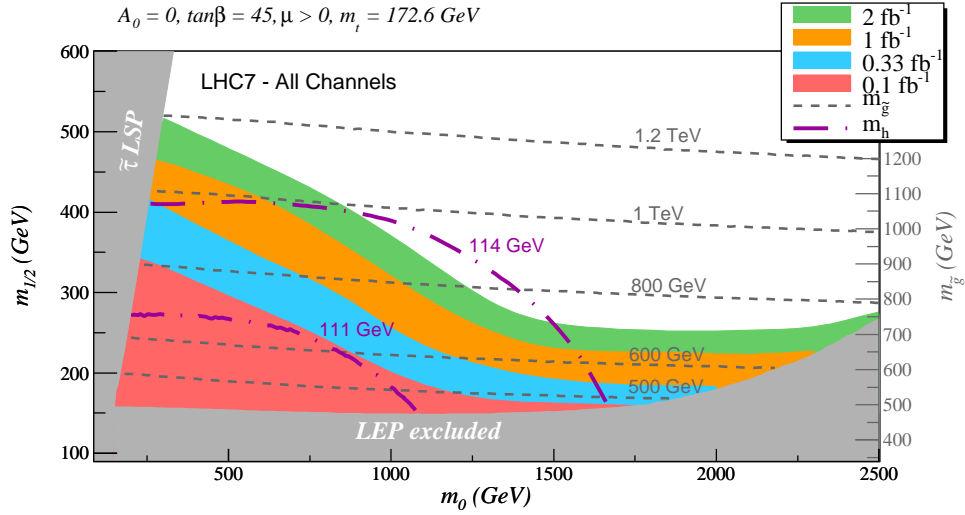


Figure 2: The optimized SUSY reach of LHC7 for different integrated luminosities combining the different channels described in the text. The fixed mSUGRA parameters are $A_0 = 0$, $\tan\beta = 45$ and $\mu > 0$. Gluino mass contours (dashed, dark grey) are shown by the dashed, dark grey curves. Higgs mass contours (dash-dotted purple) are also shown for $m_h = 111$ and 114 GeV. The shaded grey area is excluded due to stau LSPs (left side of figure) or no electroweak symmetry breaking (right side of figure), while the shaded grey area marked “LEP excluded” is excluded by non-observation of a particle signal from LEP2 searches.

We emphasize here that the reach in Fig. 2 has been obtained at LO using the rates as given by Isajet. If instead, we scale the $\tilde{q}\tilde{q} + \tilde{q}\tilde{g} + \tilde{g}\tilde{g}$ cross section to its NLO value as given by Prospino [14] (the scaling factor varies between 1.3-2.5 depending on where we are in the plane), and scale the SM background cross sections where available to their NLO values using MCFM [17], the reach in $m_{1/2}$ is *increased* by about 5% for low m_0 values, and by as much as 15-20% for high values of m_0 . We have checked that if we also include fluctuations of the background using the procedure used by ATLAS [18], and include a 50% systematic uncertainty [19] that we add in quadrature to the statistical uncertainty of the background, the reach in $m_{1/2}$ is *reduced* from its value in Fig. 2, the reduction being just a few percent for an integrated luminosity of 1 fb^{-1} , and almost 25% for 100 pb^{-1} at low values of m_0 .

In Fig. 3, we show the optimized reach restricted to the $n(\ell) = 0$, $n(b) \geq 0$ channel. We see that the 0ℓ multi-jet + E_T^{miss} channel – which has the largest cross section of all the signal channel – essentially saturates the reach, except for tiny regions at large m_0 and integrated luminosities $\geq 1 \text{ fb}^{-1}$.

While the greatest LHC reach occurs in the multi-jet+ E_T^{miss} channel, it is important to note that even for very low integrated luminosities there should be a signal in several different channels if the new physics is supersymmetry as manifested by the mSUGRA model framework. With this in mind, in Fig. 4 we compare the 1 fb^{-1} optimized reaches in the $n(\ell) = 1$, OS , SS , 3ℓ channels (all with $n(b) \geq 0$) against the $n(b) \geq 2$ channel (with $n(\ell) = 0$). The presence of the multilepton channels not only will lend confidence

that one is indeed seeing SUSY cascade decays, but also sparticle mass information may be extracted, *e.g.* the $m(\ell^+\ell^-)$ mass edge [20, 7] conveys information on the $m_{\tilde{Z}_2} - m_{\tilde{Z}_1}$ mass difference, or on sleptons masses.

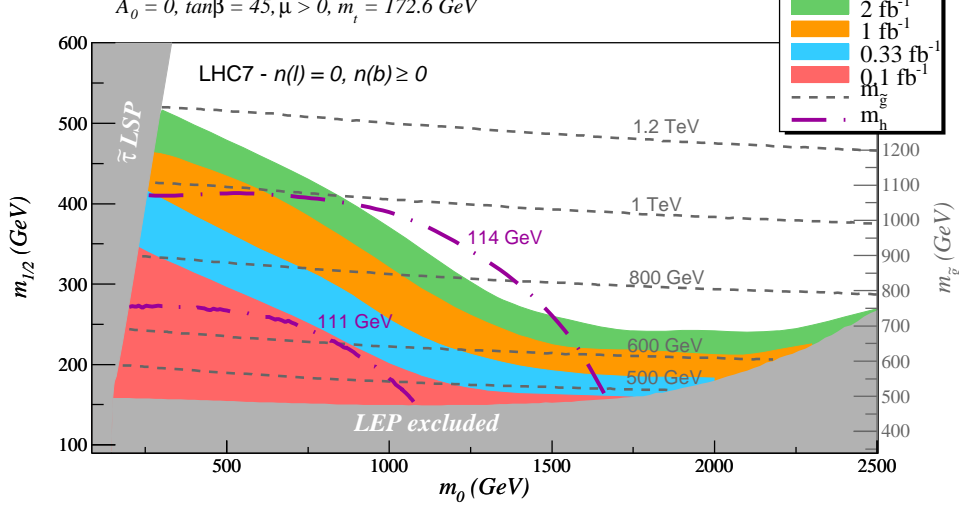


Figure 3: The optimized SUSY reach of LHC7 with different integrated luminosities for the $n(\ell) = 0, n(b) \geq 0$ channel. The fixed mSUGRA parameters are $A_0 = 0, \tan\beta = 45$ and $\mu > 0$. Gluino mass contours (dashed, dark grey) are shown by the dashed, dark grey curves. Higgs mass contours (dash-dotted purple) are also shown for $m_h = 111$ and 114 GeV. The shaded grey area is excluded due to stau LSPs or no electroweak symmetry breaking, while the shaded area marked “LEP excluded” is excluded by direct LEP bounds on sparticle masses.

3.1 Identifying the light Higgs boson in SUSY cascade events at LHC7

We note that while discovery of SUSY particles may be possible during the first run of the LHC, detection of a SM-like Higgs boson using conventional production and decay modes will require much higher integrated luminosity, primarily because an observable signal occurs only via its sub-dominant decay modes. However, it is also possible to detect the lightest SUSY Higgs boson via its dominant $h \rightarrow b\bar{b}$ decay when it is produced via cascade decays of gluinos and squarks [21]. The idea is to produce \tilde{g} and \tilde{q} at a large rate, and look for $\tilde{q} \rightarrow q\tilde{Z}_2$ or $\tilde{g} \rightarrow q\tilde{q}\tilde{Z}_2$ production followed by $\tilde{Z}_2 \rightarrow \tilde{Z}_1 h$ decay, in a E_T^{miss} event sample designed to pick our SUSY events over SM backgrounds. If $m_{\tilde{Z}_2} > m_{\tilde{Z}_1} + m_h$, then the latter decay mode becomes kinematically allowed and usually dominates the \tilde{Z}_2 decay branching fractions. Then, one might search for a $b\bar{b}$ mass bump within the SUSY signal sample.

As an example, we generate gluino and squark pair production events at the mSUGRA point $m_0, m_{1/2}, A_0, \tan\beta, \text{sign}(\mu) = 330 \text{ GeV}, 330 \text{ GeV}, 0, 10, (+)$, and apply the cuts:

- $n(j) \geq 4, n(b) \geq 2, n(l) = 0, pT(j_1) > 100 \text{ GeV}, S_T > 0.2$ and $E_T^{\text{miss}} > 250 \text{ GeV}$

For this set of cuts $t\bar{t} + \text{jets}$ is the dominant background, which is partially reduced by the isolated lepton veto. We construct the di- b -jet invariant mass of the two hardest

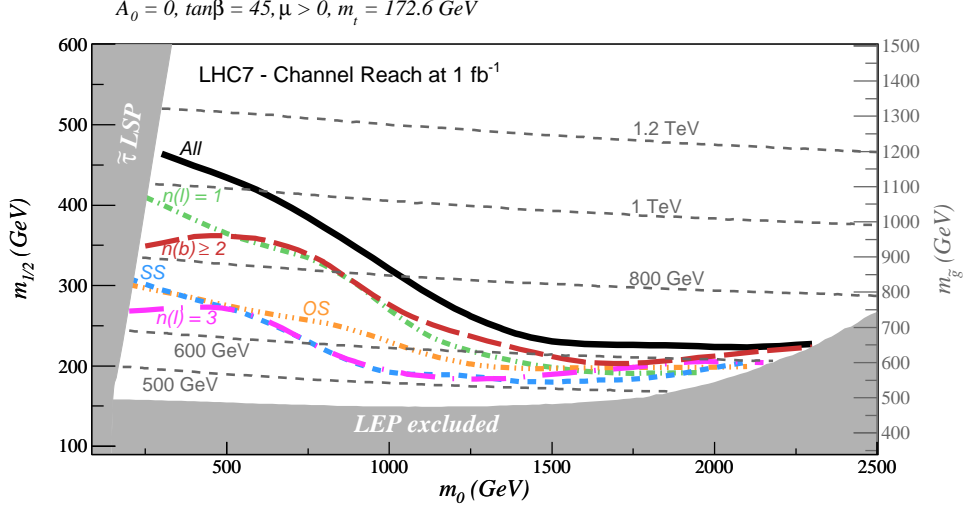


Figure 4: The optimized reach for 1 fb^{-1} restricted to multileptons ($n(\ell) = 1$, OS , SS , 3ℓ , with $n(b) \geq 0$) or multi b-jets ($n(b) \geq 2$, with $n(\ell) = 0$) channels. The fixed mSUGRA parameters are $A_0 = 0$, $\tan\beta = 45$ and $\mu > 0$. Gluino mass contours (dashed, dark grey) are shown by the dashed, dark grey curves. The shaded grey area is excluded due to stau LSPs or no electroweak symmetry breaking, while the shaded area marked “LEP excluded” is excluded by direct LEP bounds on particle masses.

b -jets, and plot the distribution in Fig. 5. The signal plus background is shown by the red histogram, while background is shown in blue. For these hard cuts the signal stands out above background, but for only 1 fb^{-1} of integrated luminosity, there would be only about 3 signal events in the peak region. However, as more events are gathered, gradually a signal should begin clustering in the vicinity of the Higgs mass. If the LHC7 run goes exceptionally well and $2\text{--}3 \text{ fb}^{-1}$ of integrated luminosity is accrued, or if the data from ATLAS and CMS detectors can be effectively combined, then evidence for the Higgs in SUSY signal events might be found. For higher values of $m_{1/2}$ and m_0 , the signal should decrease, and more integrated luminosity will be required. If $m_{1/2}$ is lowered, then the $\tilde{Z}_2 \rightarrow \tilde{Z}_1 h$ mode will close. There will then be no Higgs boson signal as \tilde{Z}_2 instead decays via $\tilde{Z}_2 \rightarrow \tilde{Z}_1 Z$ or possibly $\tilde{Z}_2 \rightarrow \tilde{f} f$ (f is a SM fermion) or via 3-body decay modes, leading to other signatures that may be searched for.

4. Early SUSY discovery at $\sqrt{s} = 7 \text{ TeV}$ without utilizing E_T^{miss}

In previous analyses [5, 6, 7], it has been shown that even without utilizing E_T^{miss} and with an integrated luminosity of just $\sim 0.1 \text{ fb}^{-1}$, experiments at LHC10 or LHC14 could detect SUSY signals in both the multimuon as well as in the acollinear dijet channels, for parameter regions beyond the reach of the Fermilab Tevatron. Our objective in this section is to check that this is still possible for the case of LHC7, and if so, delineate the portion of mSUGRA parameter space can be explored.

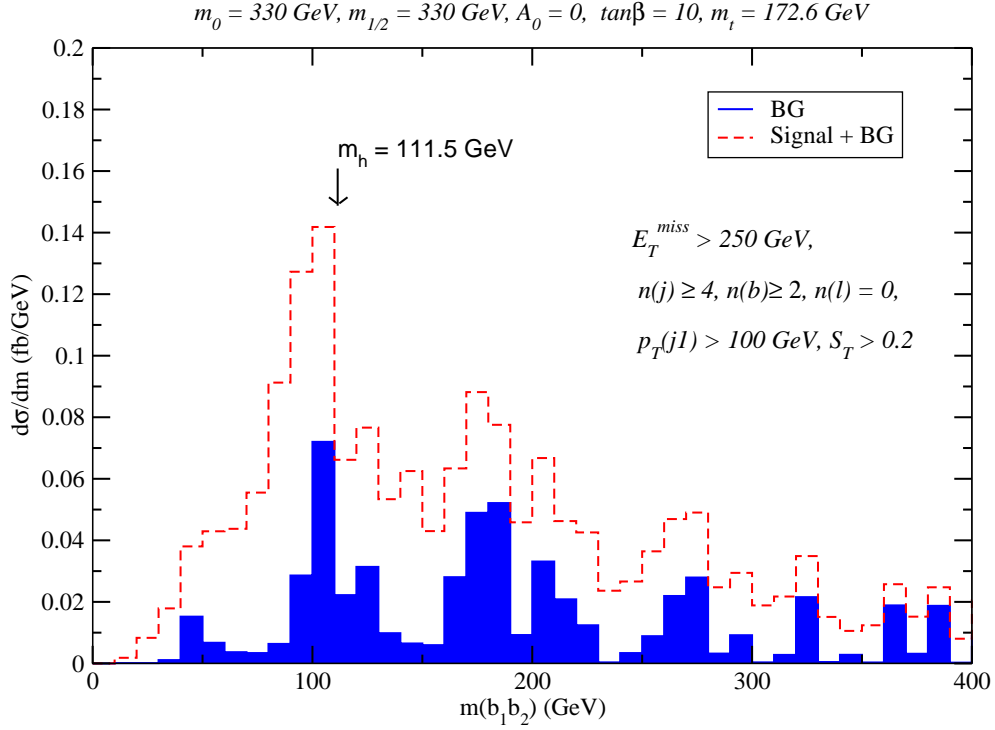


Figure 5: Invariant mass of di- b -jet pair from SUSY plus BG events (red histogram) and SM background, after cuts listed in the text, for the mSUGRA point $m_0, m_{1/2}, A_0, \tan\beta, \text{sign}(\mu) = 330 \text{ GeV}, 330 \text{ GeV}, 0, 10, (+)$.

4.1 Multilepton channels

For early SUSY discovery using multiple isolated leptons in lieu of E_T^{miss} , we use the following set of cuts:

C_{lep} :

- Jet cuts: $n(\text{jets}) \geq 4$ with $E_T(j_1) \geq 100 \text{ GeV}$, $E_T(j) \geq 50 \text{ GeV}$,
- $S_T \geq 0.2$,
- Z-veto cuts: $10 \text{ GeV} \leq m(\ell^+\ell^-) \leq 75 \text{ GeV}$ or $m(\ell^+\ell^-) \geq 105 \text{ GeV}$ (for OS/SF dileptons only)

We show results for the conservative case of $\ell = \mu$ only, as well as for the more optimistic case $\ell = e$ or μ , to cover the likely possibility that electrons will also be identifiable in the early stage of LHC7. The *multi-lepton channel* is further divided in opposite sign dileptons, same sign dileptons and trileptons.

In Fig. 6, the LHC discovery reach for the *a)* OS dimuon, *b)* SS dimuon and *c)* trimuon signals with no E_T^{miss} cuts are shown by the colored shaded regions for 0.1, 0.33, 1 and 2 fb^{-1} of integrated luminosity. We have checked that the trimuon signal in frame *c)* is below the 5 event level for all but one scanned point located in the tiny orange triangle in the $m_0 - m_{1/2}$ plane in the last frame of the figure, even for an integrated luminosity

as high as 1 fb^{-1} . Thus, unlike the situation at LHC10 [7] where the highest multimMuon reach was obtained in the trimuon channel, *there is no reach in this channel at LHC7*.

If reliable electron ID in jetty events is possible early in the LHC run and we can include isolated e s as well as μ s, the signal in the trilepton channel is roughly eight times larger than with muons alone (assuming the same acceptance and detection efficiency for electrons and muons). In this case, the reach via trileptons again exceeds the reach for OS and SS dileptons for integrated luminosity values of $\sim 1 \text{ fb}^{-1}$.

The following other features from the figure are worth noting.

1. Due to the reduced cross-sections, there is no reach for 0.1 fb^{-1} in the multi-muon channels. As in the case of LHC10, the larger signal cross section for OS dimuons implies that the earliest reach is obtained in the OS dimuon channel, but the SS dimuon channel with its larger $S : B$ ratio, yields the greater reach (in $m_{\tilde{g}}$), which, at its maximum extends up to $m_{\tilde{g}} \sim 550 \text{ GeV}$ for $m_{\tilde{g}} \lesssim m_{\tilde{q}}$, with 1 fb^{-1} of integrated luminosity. After the C_{lep} cut, $t\bar{t}$ and $Z^*/\gamma^*(\rightarrow l\bar{l})$ are the main SM backgrounds for OS dileptons, while the SS dilepton background is dominated by $t\bar{t}$ only.
2. When electrons are included in the multilepton channels, the reach increases considerably, with a tiny region of parameter space being accessible even for 0.1 fb^{-1} of integrated luminosity. The large increase in the trilepton channel (due to the inclusion of electrons) and its tiny background (dominated by $t\bar{t}$ and $t\bar{t}Z$) makes this the best channel for larger integrated luminosities. At the 1 fb^{-1} level, the reach extends up to $m_{\tilde{g}} \sim 680 \text{ GeV}$ for $m_{\tilde{g}} \lesssim m_{\tilde{q}}$. Also, larger values of m_0 become accessible.
3. While the reach in the OS and SS channels (both for dimuons and dileptons) are background limited, the trilepton reach is limited by its signal cross-section, with a total background $\lesssim 0.5 \text{ fb}$.

4.2 Acollinear dijet channel

The discovery potential of the acollinear dijet channel, suggested as a discovery mode in Ref. [6], is shown in Fig. 7. We adopt the set of cuts:

C_{dijet} :

- $n(\text{jets}) = 2$,
- $E_T(j) \geq 50 \text{ GeV}$,
- $E_T(j_1) + E_T(j_2) \geq 650 \text{ GeV}$,
- $\alpha \equiv E_T(j_2)/m(j_1 j_2) > 0.1$,
- $\Delta\phi(j_1, j_2) < 2.4$,
- number of isolated leptons $n(\ell) = 0$.²

²Even if the experiments cannot readily identify electrons because jets fake an electron at an unacceptable rate in the early stage of running, this will not preclude the possibility of vetoing electrons.

	0.1 fb ⁻¹	0.33 fb ⁻¹	1 fb ⁻¹	2 fb ⁻¹
$\sqrt{s} = 7$ TeV	0.8 TeV	0.9 TeV	1.1 TeV	1.2 TeV
$\sqrt{s} = 10$ TeV	1.0 TeV	1.1 TeV	1.4 TeV	1.5 TeV
$\sqrt{s} = 14$ TeV	1.3 TeV	1.6 TeV	1.8 TeV	2.0 TeV

Table 2: The optimized SUSY reach of the LHC within the mSUGRA model expressed in terms of the gluino mass for integrated luminosity values of 0.1, 0.33, 1 and 2 fb⁻¹ at $\sqrt{s} = 7$ TeV, 10 TeV and 14 TeV, assuming $m_{\tilde{q}} \sim m_{\tilde{g}}$. The results for 10 and 14 TeV are obtained from Ref. [7]

As expected, this channel is most effective at low m_0 where \tilde{q}_R decays mainly via $\tilde{q}_R \rightarrow q\tilde{Z}_1$. The signal rapidly degrades as m_0 increases, where squarks and gluinos then decay to multiple jets and/or leptons via SUSY cascades decays [22]. The reach extends up to $m_{\tilde{g}} \sim 900$ GeV for 1 fb⁻¹ and low values of m_0 . As at LHC10 [7], this channel complements the multi-lepton channel in that for small m_0 , the dijet reach extends to larger values of $m_{1/2}$ whereas the multilepton channel probes larger values of m_0 .

5. Summary and conclusions

With the first pp collisions at $\sqrt{s} = 7$ TeV, the era of LHC exploration of the TeV energy scale has begun. In this paper, we have calculated the LHC7 reach for supersymmetric particles assuming an integrated luminosity in the vicinity of ~ 1 fb⁻¹.

The good agreement that the CMS and Atlas collaborations find [8, 9] between Monte Carlo simulations and the very early LHC data at $\sqrt{s} = 0.9$ and 2.36 TeV indicates that analyses including reliable E_T^{miss} resolution as well as electron ID may be viable very early. Our main result is shown in Fig. 2: we find that with just ~ 1 fb⁻¹ of data – as anticipated in the first run of the LHC – gluinos up to 1.1 TeV (650 GeV) should be accessible if $m_{\tilde{q}} \sim m_{\tilde{g}}$ ($m_{\tilde{q}} \gg m_{\tilde{g}}$). Such a large reach for SUSY, even with half the design energy and very low integrated luminosity, illustrates the sheer discovery power of a three-and-a-half fold increase of the CM energy of the LHC over the Tevatron.

Our results are succinctly summarized in Table 2 where we show the optimized reach of the LHC at $\sqrt{s} = 7$ TeV and also at its design energy of 14 TeV, taking $m_{\tilde{q}} \sim m_{\tilde{g}}$. While the current plan is to ramp the energy to 14 TeV after the machine upgrade following the first run, it is entirely possible that the LHC may have to be run at a lower energy of 10–13 TeV if the required training of the magnets cannot be completed during the shutdown. To facilitate the interpolation of the LHC SUSY reach at these slightly reduced energies, we have also included the reach of LHC10 from Ref. [7] in Table 2.

Ultimately, the proper utilization of E_T^{miss} in SUSY searches will require an understanding of the high energy tail of its distribution at values well beyond where reconstruction algorithms have been tested (even allowing for the scaling with the increased CM energy to 7 TeV). Taking a conservative view that it may well take time (and data) before detectors are understood well enough for E_T^{miss} analyses to be reliably performed, we have also shown the LHC7 reach using multimuons, multileptons and dijets channels, with no E_T^{miss} cuts. In this case, the LHC7 reach is of course more limited, but still substantial: it extends up

to $m_{\tilde{g}} \sim 550$ GeV (680 GeV) in the dimuon (dilepton) channel for 1 fb^{-1} of integrated luminosity and, even if squarks are very heavy, up to 500-600 GeV in the trilepton channel. In the case where $m_{\tilde{q}} \sim m_{\tilde{g}}$, the LHC7 reach in the acollinear dijet channel, extends to $m_{\tilde{g}} \sim 900$ GeV for 1 fb^{-1} .

To conclude, the long-awaited search for physics beyond the SM has begun in earnest at the LHC. Although the machine is operating at just half its design energy, at least within the context of discovery of squarks and gluinos of supersymmetry, LHC experiments in their first run should be able to probe far beyond current limits whether or not reliable E_T^{miss} determination or electron ID is available. If, as it appears, E_T^{miss} can be reliably used early on in LHC analyses, experiments should be able to access SUSY gluinos and squarks as heavy as ~ 1 TeV with just 1 fb^{-1} of data, for the case of comparable sparticle masses.

Acknowledgments

We thank Graham Ross for urging us to perform this study. We thank Michael Schmitt and Sridhar Dasu for helpful discussions. We thank M. Mangano for helpful comments on the MLM matching algorithm. We also thank JoAnne Hewett for urging us to consider how the systematic error on the data-driven background estimates would affect the reach. XT thanks the UW IceCube collaboration for making his visit to the University of Wisconsin, where much of this work was done, possible. This research was supported in part by the U.S. Department of Energy, by the Fulbright Program and CAPES (Brazilian Federal Agency for Post-Graduate Education).

References

- [1] The Minimal Supersymmetric Standard Model commonly used today was introduced by, S. Dimopoulos and H. Georgi, *Nucl. Phys. B* **193** (1981) 150; N. Sakai, *Z. Physik C* **11** (1981) 153; for reviews of SUSY phenomenology, see H. Baer and X. Tata, *Weak Scale Supersymmetry: From Superfields to Scattering Events*, (Cambridge University Press, 2006); M. Drees, R. Godbole and P. Roy, *Theory and Phenomenology of Sparticles*, (World Scientific, 2004); P. Binetruy, *Supersymmetry* (Oxford University Press, 2006); S. P. Martin, hep-ph/9709356.
- [2] H. Baer, X. Tata and J. Woodside, *Phys. Rev. D* **45** (1992) 142; H. Baer, C. H. Chen, F. Paige and X. Tata, *Phys. Rev. D* **52** (1995) 2746 and *Phys. Rev. D* **53** (1996) 6241; H. Baer, C. H. Chen, M. Drees, F. Paige and X. Tata, *Phys. Rev. D* **59** (1999) 055014; H. Baer, C. Balázs, A. Belyaev, T. Krupovnickas and X. Tata, *J. High Energy Phys.* **0306** (2003) 054; see also, S. Abdullin and F. Charles, *Nucl. Phys. B* **547** (1999) 60; S. Abdullin *et al.* (CMS Collaboration), *J. Phys. G* **28** (2002) 469 [hep-ph/9806366]; B. Allanach, J. Hetherington, A. Parker and B. Webber, *J. High Energy Phys.* **08** (2000) 017; E. Izaguirre, M. Manhart and J. Wacker, arXiv:1003.3886 (2010).
- [3] A. Chamseddine, R. Arnowitt and P. Nath, *Phys. Rev. Lett.* **49**, 970 (1982); R. Barbieri, S. Ferrara and C. Savoy, *Phys. Lett B* **119**, 343 (1982); N. Ohta, *Prog. Theor. Phys.* **70**, 542 (1983); L. Hall, J. Lykken and S. Weinberg, *Phys. Rev. D* **27**, 2359 (1983).
- [4] Local supersymmetry was first considered by D. Volkov and V. Soroka, *JETP* **18** (1973) 312 and subsequently developed by many authors. The couplings of matter and gauge multiplets

- to supergravity were completely worked out by E. Cremmer, S. Ferrara, L. Girardello and A. van Proeyen, *Nucl. Phys. B* **212** (1983) 413.
- [5] H. Baer, H. Prosper and H. Summy, *Phys. Rev. D* **77** (2008) 055017; H. Baer, A. Lessa and H. Summy, *Phys. Lett. B* **674** (2009) 49; J. Edsjo, E. Lundstrom, S. Rybeck and J. Sjolín, *J. High Energy Phys.* **1003** (2010) 054.
 - [6] L. Randall and D. Tucker-Smith, *Phys. Rev. Lett.* **101** (2008) 221803.
 - [7] H. Baer, V. Barger, A. Lessa and X. Tata, *J. High Energy Phys.* **0909** (2009) 063.
 - [8] V. Khachatryan *et al.* (CMS collaboration), *J. High Energy Phys.* **1002** (2010) 041; A. Safonov (CMS collaboration), arXiv:1003.4038 (2010); see also CMS reports CMS-PAS-JME-10-002, CMS-PAS-EGM-10-001 and CMS-PAS-PFT-10-001.
 - [9] G. Aad *et al.* (Atlas collaboration), arXiv:1003.3124 (2010).
 - [10] For perspective on SM background to SUSY signals, see *e.g.* H. Baer, V. Barger and G. Shaughnessy, *Phys. Rev. D* **78** (2008) 095009; M. Mangano, *Eur. Phys. J. C* **59** (2009) 373. H. Baer, arXiv:0901.4732.
 - [11] T. Sjostrand, S. Mrenna and P. Skands, *J. High Energy Phys.* **0605** (2006) 026.
 - [12] M. Mangano, M. Moretti, F. Piccinini, R. Pittau and A. Polosa, *J. High Energy Phys.* **0307** (2003) 001.
 - [13] ISAJET, by H. Baer, F. Paige, S. Protopopescu and X. Tata, hep-ph/0312045; see also H. Baer, J. Ferrandis, S. Kraml and W. Porod, *Phys. Rev. D* **73** (2006) 015010.
 - [14] W. Beenakker, R. Hopker, M. Spira, hep-ph/9611232 (1996).
 - [15] A. Box and X. Tata, *Phys. Rev. D* **77** (2008) 055007 and *Phys. Rev. D* **79** (2009) 035004.
 - [16] The Isajet 7.79 manual is available at
<http://www.nhn.ou.edu/~isajet/>
 .
 - [17] MCFM, by J. Campbell and R. K. Ellis. See R. K. Ellis, Nucl. Phys. Proc. Suppl. **160** (2006) 170.
 - [18] G. Aad *et al.* (Atlas collaboration), arXiv:0901.0512 (2009).
 - [19] G. Aad *et al.* (Atlas collaboration), ATLAS-PHYS-PUB-2009-084 (2009).
 - [20] H. Baer, K. Hagiwara and X. Tata, *Phys. Rev. D* **35** (1987) 1598; H. Baer, D. Dzialo-Karatas and X. Tata, *Phys. Rev. D* **42** (1990) 2259; H. Baer, C. Kao and X. Tata, *Phys. Rev. D* **48** (1993) 5175; H. Baer, C. H. Chen, F. Paige and X. Tata, *Phys. Rev. D* **50** (1994) 4508; I. Hinchliffe *et al.* *Phys. Rev. D* **55** (1997) 5520; H. Bachacou, I. Hinchliffe and F. Paige, *Phys. Rev. D* **62** (2000) 015009; See also, ATLAS collaboration, *Atlas Physics and Detector Performance Technical Design Report LHCC 99-14/15*, and *Expected Performance of the ATLAS Experiment: Detector, Trigger and Physics*, CERN-OPEN-2008-020; CMS Collaboration, *Physics Technical Design Report*, V. II, CERN/LHCC 2006-021.
 - [21] H. Baer, M. Bisset, X. Tata and J. Woodside, *Phys. Rev. D* **46** (1992) 303; C. Balázs, A. Belyaev, T. Krupovnickas and X. Tata, Ref. [2]; see also, ATLAS TDR, Ref. [20] and CMS Physics TDR, Ref. [20].

- [22] H. Baer, J. Ellis, G. Gelmini, D. V. Nanopoulos and X. Tata, *Phys. Lett.* **B 161** (1985) 175; G. Gamberini, *Z. Physik* **C 30** (1986) 605; H. Baer, V. Barger, D. Karatas and X. Tata, *Phys. Rev.* **D 36** (1987) 96.
- [23] U. Chattopadhyay, A. Datta, A. Datta, A. Datta and D. P. Roy, *Phys. Lett.* **B 493** (2000) 127; P. G. Mercadante, J. K. Mizukoshi and X. Tata, *Phys. Rev.* **D 72** (2005) 035009; S. P. Das, A. Datta, M. Guchait, M. Maity and S. Mukherji, *Eur. Phys. J.* **C 54** (2008) 645; R. Kadala, P. G. Mercadante, J. K. Mizukoshi and X. Tata, *Eur. Phys. J.* **C 56** (2008) 511.

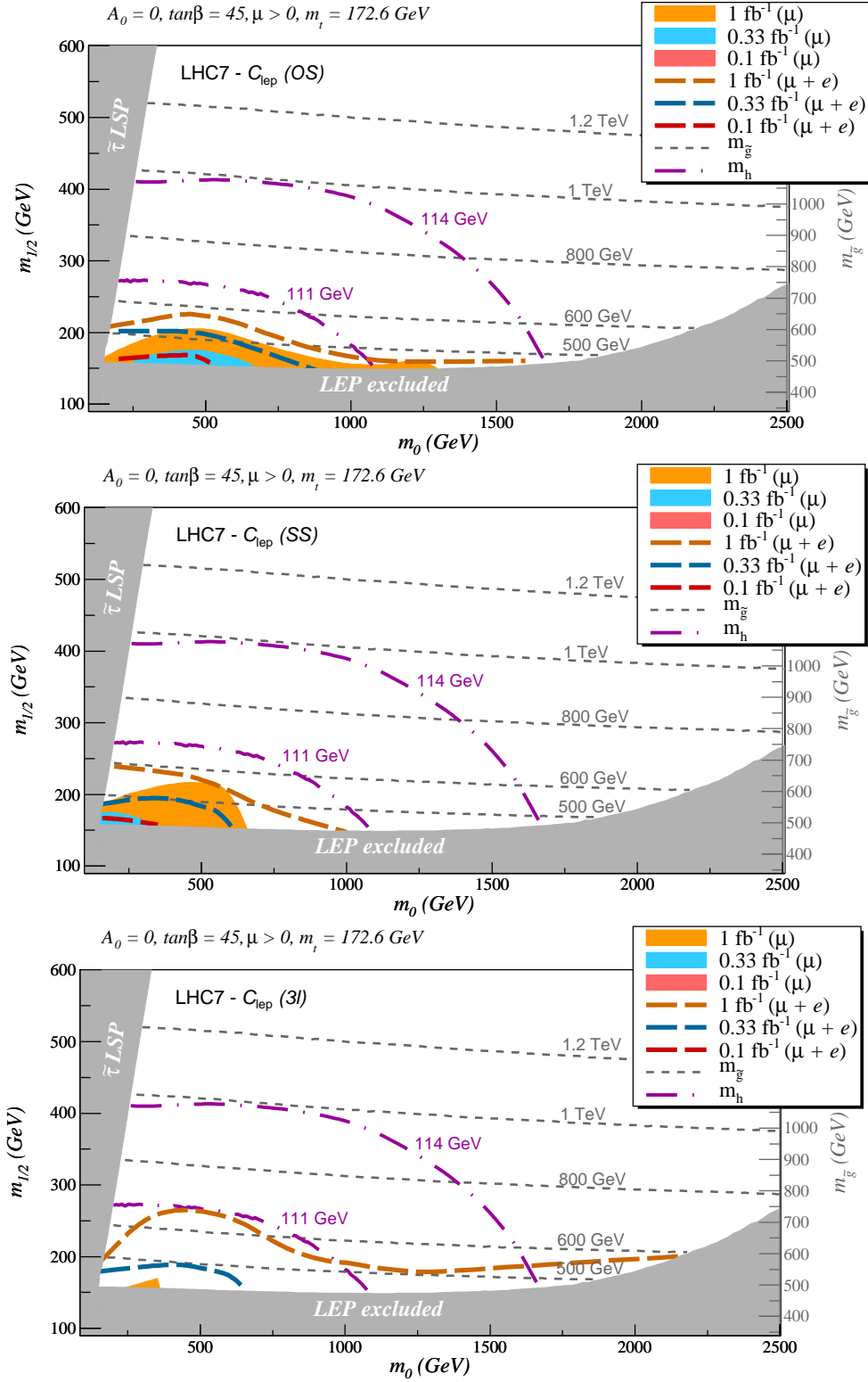


Figure 6: SUSY reach of the LHC at $\sqrt{s} = 7$ TeV for different luminosities via a) OS-dimuon (dilepton) events, b) SS-dimuon (dilepton) and a) trimuon (trilepton) events using the cuts C_{lep} for $l = \mu$ ($l = \mu, e$) introduced in the text. The fixed mSUGRA parameters are $A_0 = 0$, $\tan\beta = 45$ and $\mu > 0$. Gluino mass contours (dashed, dark grey) are shown by the dashed, dark grey curves. Higgs mass contours (dash-dotted purple) are also shown for $m_h = 111$ and 114 GeV. The shaded grey area is excluded due to stau LSPs or no electroweak symmetry breaking, while the shaded area marked “LEP excluded” is excluded by direct LEP bounds on sparticle masses.

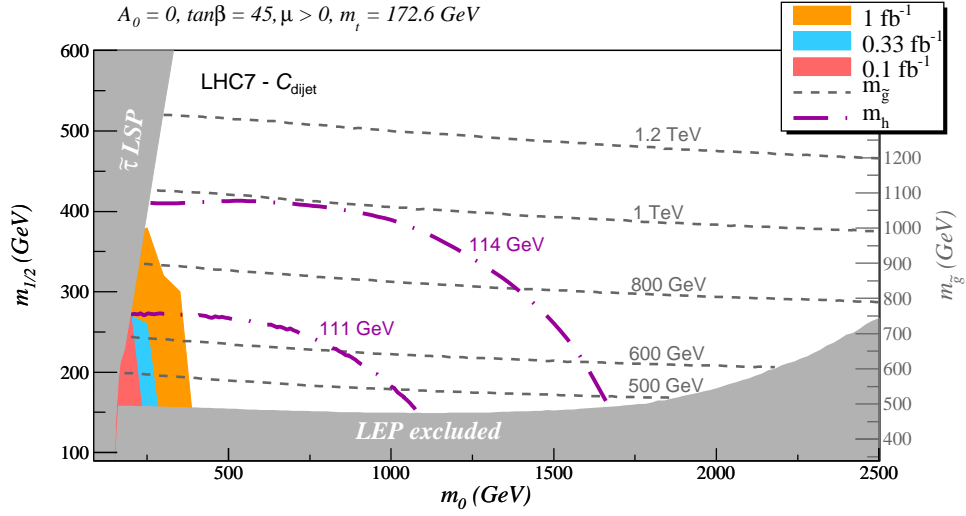


Figure 7: SUSY reach of the LHC at $\sqrt{s} = 7 \text{ TeV}$ for different luminosities via the dijet channel using the cuts C_{dijet} . The fixed mSUGRA parameters are $A_0 = 0$, $\tan\beta = 45$ and $\mu > 0$. Gluino mass contours (dashed, dark grey) are shown by the dashed, dark grey curves. Higgs mass contours (dash-dotted purple) are also shown for $m_h = 111$ and 114 GeV . The shaded grey area is excluded due to stau LSPs or no electroweak symmetry breaking, while the shaded area marked “LEP excluded” is excluded by direct LEP bounds on sparticle masses.